JOTCS A
Journal of the Turkish Chemical Society
Section: A
Chemistry
TURKISH CHEMICAL SOCIETY

Green Preparation of Multiwalled Carbon Nanotubes-Supported Pd and Cu Nanoparticles with Novel *Vic*-dioxime Metal Complexes

Fatma Ulusal* , **Bilgehan Güzel**

Chemistry Department, Art and Science Faculty, University of Çukurova, 01330, Adana, Turkey.

Abstract: The preparation of multi-walled carbon nanotubes (MW-CNTs) supported Cu and Pd nanoparticles utilizing a supercritical carbon dioxide ($scCO_2$) deposition method were investigated. Novel *vic*-dioxime complexes of Cu(II) and Pd(II) were used as metallic precursors. The ligand used in these precursors was 4-(trifluoromethyl)aniline-*vic*-dioxide. Ligand and metal complexes were synthesized and identified with various analysis methods including ^{1}H and ^{19}F NMR, FT-IR, UV-Vis, elemental analysis and magnetic susceptibility. MW-CNTs supported Pd and Cu nanoparticles were characterized by high-resolution transmission electron microscopy (HR-TEM), X-ray diffraction (XRD) and scanning electron microscopy with EDX (SEM-EDX). SEM-EDX and HR-TEM micrographs showed a homogenous distribution of reasonably well-dispersed Cu and Pd nanoparticles on the support. The nature and crystallinity of the nano metal particles were confirmed using XRD. Crystallite sizes ranged from 7-20 nm for palladium and 20-30 nm for copper. This study demonstrated that these oxime complexes are suitable precursors for the preparation of supported nanoparticles using a supercritical carbon dioxide deposition method.

Keywords: *vic*-dioxime, metal complex, precursor, green chemistry, supercritical deposition.

Submitted: January 19, 2018. **Accepted:** October 25, 2018.

Cite this: Ulusal F, Güzel B. Green Preparation of Multiwalled Carbon Nanotubes-Supported Pd and Cu Nanoparticles with Novel Vic-dioxime Metal Complexes. JOTCSA. 2018;5(3):1249–56.

DOI: http://dx.doi.org/10.18596/jotcsa.381305.

***Corresponding author. E-mail:** fatma_ulusal@hotmail.com, **GSM:** +90539 886 81 10

INTRODUCTION

Preparation of transition metal nanoparticles such as Pd, Pt, Rh, Ru, Ni and Cu on a solid support surface gain importance due to the increasingly widespread application of nanocatalysts (1-3). In order to deposit these metals, various organic and inorganic supporting materials such as silica aerogel, carbon black, active carbon, CNT, and alumina are used. Especially carbon-containing materials are preferred due to their unique applications. Nano metal particles deposited on high surface area carbon materials are prominently used as catalysts for many reactions in a wide range. There are many methods for preparing these nanoparticles, such as microemulsion, chemical vapor deposition, modified polyol reduction, impregnation, sonochemical preparation, and deposition-precipitation has been reported (1,4-7).

Supercritical fluids (SCF) has been used in various application areas such as extraction, cosmetics, sterilization, energy, pharmaceutics, chemistry, organic synthesis, formulation, impregnation, cleaning, food, materials, waste treatment and deposition of metals on the solid materials (1,8). The deposition in supercritical fluids has recently been receiving a growing interest for its use in preparing deposited catalysts. This method includes the dissolving of a precursor (is usually a metalorganic compound) in an SCF and the subsequent exposure of the support material to this supercritical precursor solution. There are currently very few precursors used that are known to have the necessary characteristics for successful deposition in SCF. These include acetylacetonate, hexamethyl triethylene, hexamethylene glycol dimethyl ether, tetramethyl heptanedionate, cyclooctadiene and their derivatives (1, 9-12). We have proved that bipyridyl, phenanthroline, and oximes can also be used in a supercritical deposition with our previous studies (1,13).

In our previous studies, we have contributed to the literature by using new precursors that can be used in the $scCO_2$ deposition technique. Pd(II) complexes of *vic*-dioxime ligands were prepared and used for Pd deposition on alumina in the $scCO_2$ medium for application in Suzuki-Miyaura reaction (1). In another study, the Pd(II) complex of the bipyridyl ligand was used to prepare Pd/MW-CNT in the $scCO_2$ medium. The prepared catalyst was then used for hydrogen storage (13). In this paper, novel fluorous *vic*-dioxime ligand and its Cu(II) and Pd(II) complexes soluble in supercritical carbon dioxide were synthesized. MW-CNTs supported Pd and Cu metallic nanoparticles were prepared with $scCO_2$ deposition technique by hydrogen-assisted chemical reduction method. We investigated the properties of Pd and Cu loaded MW-CNTs by HR-TEM, SEM-EDX, and XRD.

MATERIALS AND METHODS

All chemicals were supplied from Sigma Aldrich and used as obtained without further purification. Multiwall carbon nanotubes were used had the following average dimensions: O.D. xL (6-9 nm x5 μm), diameter (mode, 5.5 nm; median, 6.6 nm). The complexes and ligands have been characterized by the spectroscopic techniques listed below and have been compared with the reported characterizations of analogous compounds. FT-IR spectra of compounds were recorded on a Thermo FT-IR spectrometer; Smart ITR diamond attenuated total reflection (ATR). Elemental analyses (C, N, H) were recorded on a Thermo Scientific Flash 2000, CHNS elemental analyses apparatus. ^{1}H and ^{19}F NMR spectra were recorded on a Bruker AVANCE-500 (in $CHCl_3$ and DMSO). Electronic spectra were obtained on a Perkin Elmer Lambda 25 UV spectrophotometer. Magnetic susceptibilities of metal complexes were determined on a Sherwood Scientific Magnetic Susceptibility balance (Model MK1) using $CuSO_4.5H_2O$ as a calibration standard at room temperature; diamagnetic corrections were calculated from Pascal's constants. The separation and washing of the MW-CNTs by precipitation were performed with a Serico 80-2 centrifuge machine. HR-TEM spectra were recorded on Jeol 2100F HR-TEM, 200kv (high-resolution transmission electron microscopy). XRD spectra were recorded on Rigaku Miniflex CuKα, λ=0.154 nm. Scanning Electron Microscopy (SEM) images were recorded on Zeiss Supra 55. The resolution of this microscope is a working distance of 10 mm at an accelerating voltage of 10 kV. The metal/MW-CNTs nanoparticles were mounted on platinum pins with double-sided carbon tape and their corresponding SEM images were recorded. Elemental analysis was obtained from the EDAX Genesis EDS system.

Preparation of ligands and complexes

Synthesis of 4-(trifluoromethyl) aniline-*vic*-dioxime [4TFVD]: As shown in Figure 2, a solution of antimonochloroglyoxime (1.8 g, 3.5 mmol) in 40 mL of absolute ethanol at -10 °C was put in a solution of 4-(trifluoromethyl)-aniline (0.45 g, 3.5 mmol) in 20 mL of ethanol at -10 °C (14). Then the mixture was stirred for 4 hours keeping its temperature under -10 °C. When it became yellow, the pH was brought to 6 by adding 0.1 M NaOH drop-wise. Subsequently, its color turned yellowish-orange. The solvent (ethanol) was allowed to evaporate at room temperature, producing crystals, which were filtered and dried in a vacuum desiccator. The high-resolution microscope image of 4-(trifluoromethyl)aniline-vic-dioxime crystal was shown in Figure 1. Yield: 63%, m.p.: 85°C. Elemental Analysis [$C_{16}H_8F_{17}N_3O_2$]; Found 135 C, 43.48; H, 3.12; N,16.41%; calculated C, 43.73; H, 3.26; N, 17.00%; IR (ATR, mmax/cm^{-1}); 3382 (N-H), 3150 (O-H), 1627 (C=N), 1526 (C=C), 1321 (N-O), 1109(C-F), 1066(N-O); ^{1}H NMR ($CDCl_3$), δppm: 11.5(d, 2H, -OH), 8.4(s, 1H, -NH), 7.7-7.4(m, 4H, Ph), 2.1(s, 1H,=CH), ^{19}F NMR ($CDCl_3$), δ ppm: -63.6(Ph-CF_3). The yellow ligand proved insoluble in chloroform, DMSO, water and n-hexane and soluble in solvents such as THF, ethanol, and acetone. (FT-IR, ^{1}H and ^{19}F NMR spectra are given in Supporting data; S1, S2 and S3).

Figure 1. The high-resolution microscopic image of 4-(trifluoromethyl)aniline-vic-dioxime crystal.

Synthesis of bis(4-(trifluoromethyl)aniline-*vic*-dioxime) copper(II) [Cu(4TFVD)$_2$]: As shown in Figure 2, a solution of 4TFVD (2 mmol) in 15 mL of ethanol was dripped on a solution of copper(II) acetate monohydrate (1 mmol) in 10 mL of ethanol. Then, the solution was refluxed at 65 °C for 5 hours. It was allowed to cool to room temperature. Then, the precipitate was filtered, washed with ethanol and dried in a desiccator under vacuum to furnish the pure Cu oxime complex. Yield: 68.0%, m.p.:197 °C. Elemental Analysis [$C_{12}H_{20}O_4N_4Cu$]; Found C, 37.94; H, 2.05; N, 14.41%; calculated, C, 38.89; H, 2.54; N, 15.12%; IR(ATR, mmax/cm^{-1}); 3384(N-H), 3063 (C-H, Ph), 1656 (O···H–O, w), 1610 (C=N), 1513-1320 (N-O) 1106-1064 (C-F), 1012(N-O). The green complex was insoluble in chloroform, DMSO, water and n-hexane and soluble in solvents such as THF, ethanol, and acetone. (FT-IR spectrum is given in Supporting data; S4).

Synthesis of bis(4-(trifluoromethyl)aniline-*vic*-dioxime) palladium(II) [Pd(4TFVD)$_2$]: As shown in Figure 2, a solution of 4TFVD (2 mmol) in 20 mL of ethanol was dripped on a solution of palladium(II) chloride (1 mmol) in 10 mL of ethanol. For the palladium complexes, sodium acetate (0.5 g) was added to the solution. Then the mixture was refluxed at 75 °C for 4.5 hours. It was allowed to cool to room temperature. The solution was filtered, washed with ethanol and dried in a desiccator by vacuum to furnish the pure Pd-oxime complex. Yield: 98%, m.p.:225 °C. Elemental Analysis [$C_{12}H_{20}O_4N_4Pd$]; Found C, 35.90; H, 2.47; N, 13.58%; calculated, C, 36.11; H, 2.36; N,14.04%; FT-IR(ATR, mmax/cm^{-1}); 3380(N-H), 3058(C-H, Ph), 1690 (O···H–O, w), 1612(C=N), 1542(C=C), 1328 (N-O), 1165-1068 (C-F), 1015 (N-O). The yellow complex was insoluble in chloroform, DMSO, water and n-hexane and soluble in solvents such as THF, ethanol, and acetone. (FT-IR spectrum is given in Supporting data; S5).

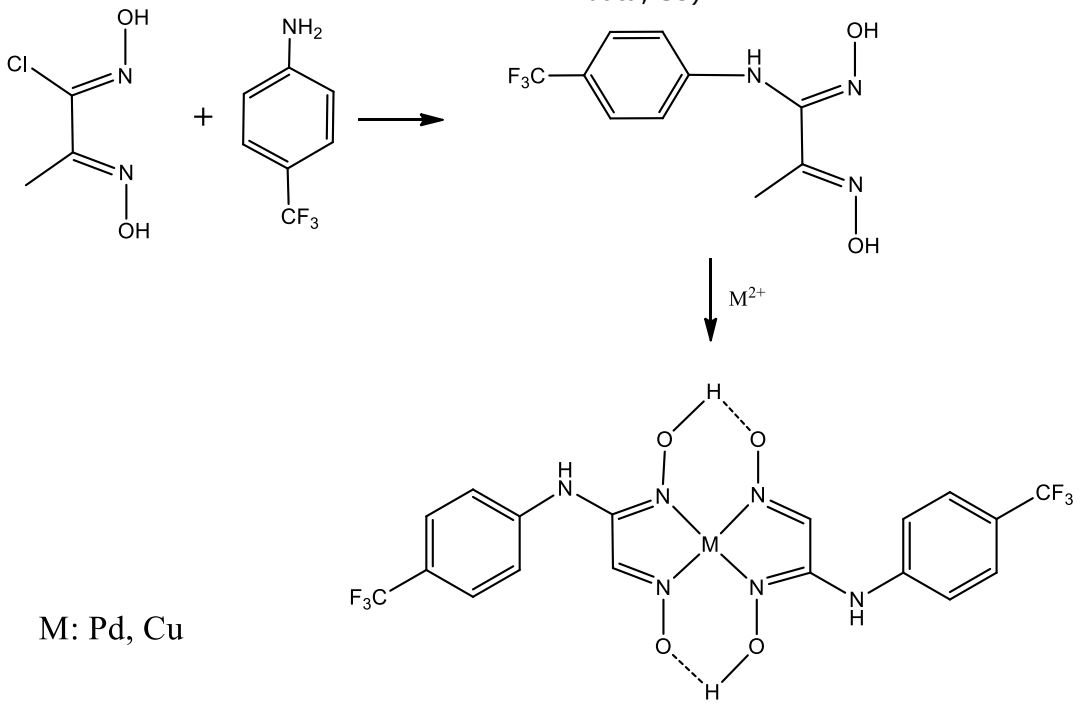

Figure 2. Synthesis reaction of 4TFVD and its metal complexes.

Determination of Solubility in Supercritical Carbon Dioxide: The solubility of the metal complexes was investigated at 276 bar and 363 K in a stainless steel reactor (an inner volume of 54 mL). The reactor was first cleaned with ethanol and CO_2. A known amount (45-50 mg) of the complex was weighed and placed inside the reactor. After the saturated supercritical solution was obtained, the solution was taken out of the vessel to a receptacle of known volume from a side vent. The gas solution was slipped through 5 mL of ethanol. The receptacle was washed with ethanol and added to the initial solution. The amount of complex solving in $scCO_2$ was measured with UV-Vis spectrophotometer.

Deposition of metals on MW-CNT

The process of preparation of the metals supported on the MW-CNTs by the $scCO_2$ deposition technique was generally carried out in 3 steps.

a. Dissolution of the precursor in $scCO_2$
b. Absorption of the precursor on MW-CNTs
c. Finally, the chemical reduction of the metal with hydrogen in $scCO_2$

A 100 mL inner volume stainless steel reactor (Amar brand) was used for the adsorption of the precursors onto an MW-CNTs and their reduction to metal particles. In a typical experiment held in $scCO_2$, the reactor was first purged by CO_2. 200 mg MW-CNT and desired amount of precursor was used to obtain 7.5% of M/MW-CNTs. After the addition of the materials to the reactor, the

system was gradually heated to 363 K by a circulating cooler/ heater. The reactor was filled with 276 bar CO_2 gas with a syringe pump (Isco 260D brand) and allowed to stand under these conditions for 1 h. Then the pressure of the vessel was reduced to 138 bar. A CO_2 (10.3 bar) and the H_2 gas mixture were prepared in a high-pressure vessel with 10 mL volume at 276 bar capacity. After stirring for 5 hours, the reactor was allowed to cool to room temperature. The gas was released very slowly and carefully. The solid that had formed was placed on a filter paper and washed with THF until it became clear. Prepared MW-CNTs supported metals nanoparticles were dried in a drying oven. The quantitative analysis of metals was done by ICP-OES. The surface properties of nanoparticles were analyzed with XRD, SEM-EDX, and HR-TEM.

RESULTS AND DISCUSSION

Synthesis of Ligands and Complexes

The oxime ligand was synthesized from fluorinated aniline and *anti* monochloroglioxime. The Cu(II) and Pd(II) complexes of *vic*-dioximes were synthesized using 4-(trifluoromethyl)aniline-*vic*-dioxime, copper(II) acetate monohydrate and palladium(II) chloride. The ligand and metal complexes were characterized by ^1H and ^{19}F NMR, FT-IR, elemental analysis, UV-Vis spectrophotometry and magnetic susceptibility.

The elemental analyses of the [4TFVD] were in agreement with the calculated values, confirming that the ligands were indeed synthesized. In the IR spectra of the ligands, the characteristic peaks appeared at 3382 cm^{-1} (N-H), 3150-3000 cm^{-1} (O-H), and 1627 cm^{-1} (C=N). The other peaks observed in the [4TFVD] spectra appeared between 1608-1520 cm^{-1} (C=C), 1320-1299 cm^{-1} (N-O), 1196-1100 cm^{-1} (C-F) and 1066-953 cm^{-1} (N-O). New bands in the IR spectra of the synthesized [4TFVD], which were not present in the starting material, belonging to the C-F bond, appeared between 1100-1200 cm^{-1}. The presence of these peaks, as well as the O-H, C=N and N-O bond, confirmed that the desired ligand was obtained. The ^1H NMR spectra of the ligands showed two overlapping singlet peaks at 11.5 ppm for [4TFVD]. This is the result of there being two different =N-OH groups present in the ligand. The other peaks that were observed in the ^1H NMR and ^{19}F NMR spectra are consistent with what is expected for these structures. The ^{19}F NMR spectrum contained the expected number of peaks. These results combine to show that the desired ligand was indeed synthesized.

The elemental analyses of the Cu(II) and Pd(II) oxime complexes are also in agreement with the calculated values (14). The physical and analytical results show a metal: ligand ratio of 1:2 for both Pd(II), and Cu(II). The reactions of the oxime ligands with Pd(II) and Cu(II) salts were yielded complexes with the overall formulas $[Cu(4TFVD)_2]$ and $[Pd(4TFVD)_2]$. In the IR spectra of the Cu(II) and Pd(II) complexes, the peaks assigned to the ν(C=N) frequency was shifted to lower frequencies than in the free ligand due to C=N--M metal coordination. For the [4TFVD] ligand, the N=C peak observed at 1627 cm^{-1} shifted to 1610 cm^{-1} for $[(Cu(4TFVD)_2]$ and 1612 cm^{-1} for $[Pd(4TFVD)_2]$. The bands corresponding to the γ(O-H) frequency observed in the free ligand was lost after complexation. Weak bands appearing around 1800–1700 cm^{-1} in the FT-IR spectra of the Cu(II) complex corresponded to intramolecular hydrogen bridges (O···H–O) which are in agreement with accepted values as these peaks generally appear between 2000-1700 cm^{-1} (14). As expected, this peak is lacking for the ligand. The magnetic susceptibility of $[(Cu(4TFVD)_2]$ was found as 1.81 μB while $[(Pd(4TFVD)_2]$ was found as 0 μB. The results showed that the geometry of these complexes is square planar.

Solubility of the Precursors

In order to understand the suitability of these complexes for using as a precursor in $scCO_2$ deposition method, a solubility test of complexes was performed. Fluorous groups are CO_2-phile and these groups increase solubility depending on elongation and increasing number of the tail. The solubility of synthesized *vic*-dioxime precursors was in agreement with commonly known precursors reported in the literature (15-17). The solubility of $Pd(4TFVD)_2$ is $7.19x10^{-5}$ g/mL CO_2 while $Cu(4TFVD)_2$ is $3.95x10^{-5}$ g/mL CO_2. The distance between the ligand and the center atom is the bigger in palladium complexes because of palladium diameter is bigger than that of copper. The distance between the ligand and the center atom is inversely proportional to the shielding of the center palladium atom by the ligands. These two effects reduce the solubility of the precursor. So the solubility of Pd precursors was almost 2 times higher than Cu precursors in $scCO_2$.

Deposition of Nanoparticle Metals

Metallic Cu and Pd were been deposited onto MW-CNTs via a supercritical fluid deposition method and H_2 assisted reduction. We also analyzed the reduction residual by FT-IR and characteristic -NH_2 peaks appear at 3300-3400 cm^{-1}. The peaks of OH (3100-3000 cm^{-1}) and C=N (1600-1650 cm^{-1}) which were present in the precursors, did not appear in this frequency.

The *vic*-dioxime-metal complexes of Pd and Cu used to deposit the metals were bis(4-(trifluoromethyl)aniline-*vic*-dioxime) palladium(II) and bis(4-(trifluoromethyl)aniline-*vic*-dioxime) copper(II). The XRD patterns of the metal support show that the metals were polycrystalline on the MW-CNT. The XRD patterns of Pd deposited on MW-CNT from $[Pd(4TFVD)_2]$ is shown in Figure 3. The main diffraction peaks of metallic Pd nanoparticles on the MW-CNTs observed were as expected. In the XRD pattern of Pd deposited on MW-CNT from $[Pd(4TFVD)_2]$,

three very sharp peaks were seen: 38.8, Pd(111); 44.8, Pd(200); and 67.3, Pd(220). These three sharp peaks referred to reflections of the face-centred cubic palladium lattice system, with the space group referred to Fm–3m (1,18). The main peak, Pd(111), was used for calculation of the average particle size of Pd nanoparticles according to the Scherrer equation. The calculated average metal particle size of Pd/MW-CNT was 7.3 nm.

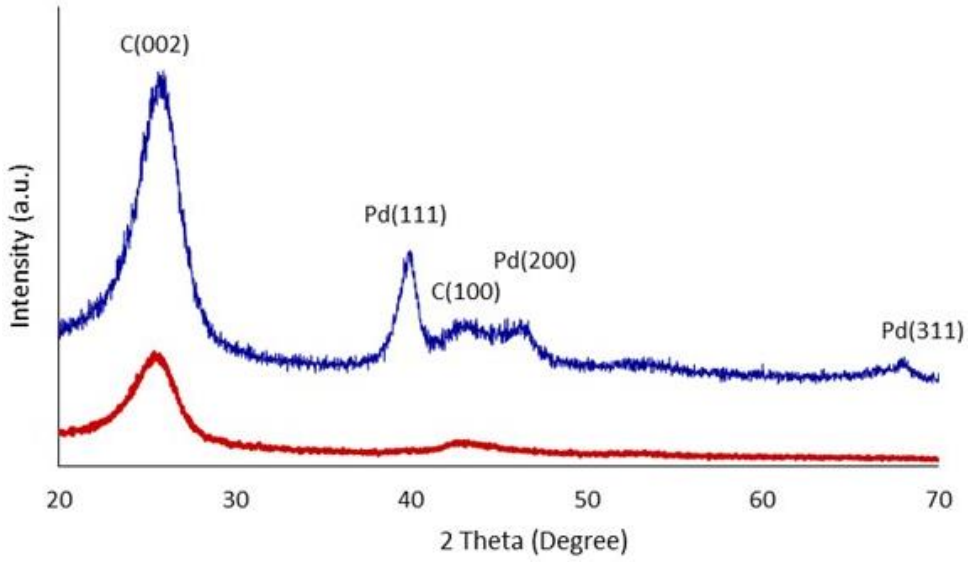

Figure 3. XRD result of (a) MW-CNTs (in red), (b) MW-CNTs supported Pd nanoparticles (in blue).

The XRD patterns of the metal/MW-CNTs show that the metals were polycrystalline on the MW-CNT for Cu as well. The XRD patterns of Cu supported on MW-CNT for [$Cu(4TFVD)_2$] is shown in Figure 4. Four very sharp diffraction peaks were observed in the XRD pattern of Cu supported on C(002): 17.0, Cu_2O(111); 36.4, Cu(111); 42.3, Cu_2O(111); 61.5, and Cu(220); 73.7 (7,19,20). It can be said that some of the Cu nanoparticles were oxidized from the obtained peaks. All peaks indicate that the Cu has a cubic crystallite structure. The main peak, Cu_2O (111), was used for calculation of the average particle size of Cu nanoparticles and average metal particle size was 27.5 nm.

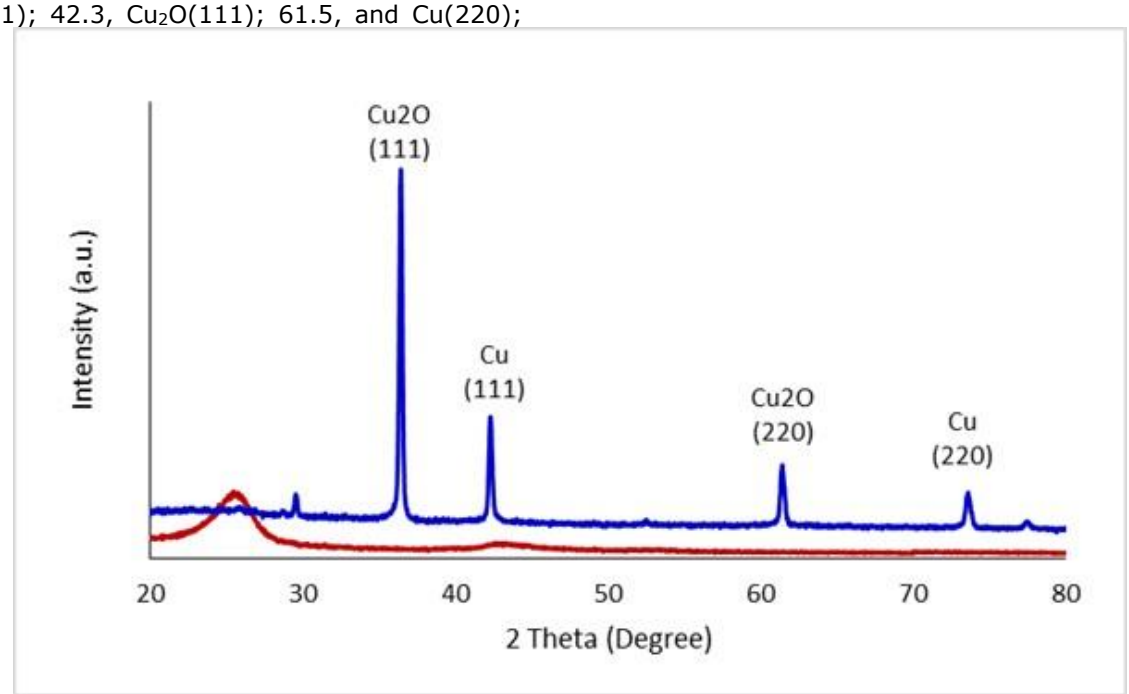

Figure 4. XRD result of (a) MW-CNTs (in red), (b) MW-CNTs supported Cu nanoparticles (in blue).

Figure 5a; it shows the HR-TEM image of the Pd/MW-CNTs obtained from the deposition of Pd on MW-CNTs by using [$Pd(4TFVD)_2$] precursor. The grey background corresponds to MW-CNTs and the black dots on this grey area are Pd nanoparticles. MW-CNTs channels are shown which are parallel to each other from TEM images. The Pd particles were distributed homogeneously on the MW-CNTs. Pd had an average particle size of 7-10 nm. We also were able to decorate MW-

CNTs with Cu nanoparticles using the same technique. HR-TEM images of Cu/MW-CNTs obtained from $[Cu(4TFVD)_2]$ are shown in Figure 5b. Cu had an average particle size of 2-10 nm.

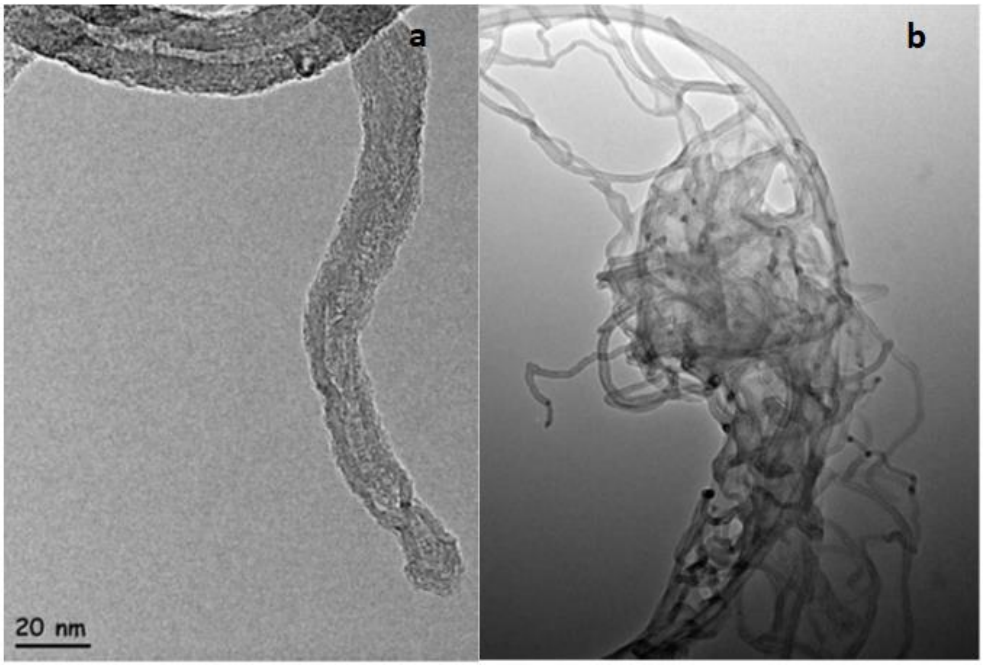

Figure 5. HR-TEM images of (a) Pd/MW-CNTs and (b) Cu/MW-CNTs.

Cu/MW-CNTs and Pd/MW-CNTs samples were analyzed through SEM with EDX. Typical SEM micrographs taken of copper and palladium deposited MW-CNTs composites created by $scCO_2$ deposition method are shown in Figure 6. The identity of the metals was determined by XRD and HR-TEM and confirmed by EDX. The metal nanoparticles were clearly visible on the surface of the MW-CNTs in the EDX spectrum, which also showed that Cu, Pd, and carbon are the major elements in the composite. While carbon peaks of high intensity were observed, the copper and palladium peaks were of low intensity. The percentage of the metal present was calculated and shown in these figures. A wide particle size distribution is observed. The experiments resulted in 6 wt.% Cu loading which accounted for 74.6% of the total Cu in the $[Cu(4TFVD)_2]$ system according to ICP-OES and EDX.

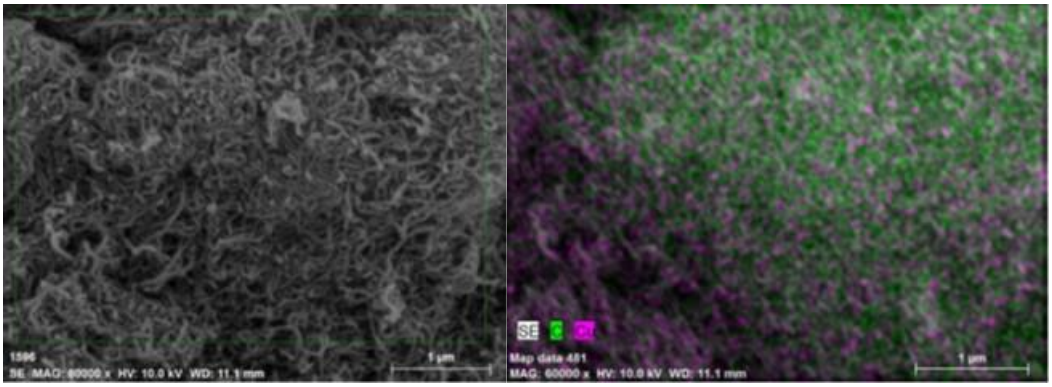

Figure 6. SEM-EDX images of Cu/MW-CNT obtained from $[Cu(4TFVD)_2]$.

The SEM micrograph of Cu/MW-CNT composites shown in Figure 7, revealed not only the homogenous distribution of copper in the MW-CNTs matrix but also Cu nanoparticles were small, devoid of large particles on the MW-CNT's surface. Homogenous distribution of the palladium MW-CNT in the matrix was also observed. Pd/MW-CNT obtained from $[Pd(4TFVD)_2]$ experiments resulted in 4 wt.% Pd loading which accounted for 49.4% of the total Pd in the system according to ICP-OES and EDX. The SEM micrograph of Pd/MW-CNT composites, shown in Figure 7, revealed not only the homogenous distribution of palladium in the MW-CNTs matrix but also Pd nanoparticles were small. However, large particles on the MW-CNT surface were also observed.

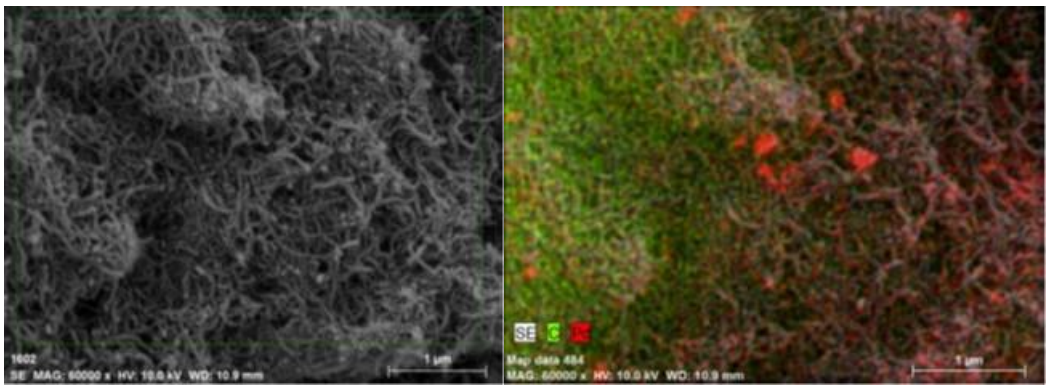

Figure 7. SEM-EDX images of Pd/MW-CNT obtained from [$Pd(4TFVD)_2$].

This study has shown that metal *vic*-dioxime complexes used as precursors can result in the successful deposition of palladium and copper nanoparticles on MW-CNTs using a $scCO_2$ medium and chemical reduction process. The results of this study regarding the suitability of these precursors will help in defining the mechanisms by which the deposition occurs. This, in turn, will allow for better future research in this area and allow for the advancement of nanocatalyst technology.

CONCLUSION

Fluorinated *vic*-dioxime metal complexes were dissolved in $scCO_2$ and deposited on MW-CNTs. The resulting materials were analyzed by HR-TEM, SEM-EDX, and XRD. These results showed that the metal particles formed were dispersed homogeneously with particles as small as 7 nm. These results show that these novel fluorous *vic*-dioxime metal precursors are a viable alternative for use in a supercritical deposition. Further research on the different isomers of *vic*-dioximes, such as the syn form, could also provide insightful information. In continuation of this research, the deposition of other various oxime derivatives on various supports and further testing on the effects of different temperature and pressures in the deposition process will be studied. The effect of different precursors on the distribution and particle size will be explained by having enough data in continuation of this research.

ACKNOWLEDGEMENTS

The authors gratefully acknowledge Prof. Dr. Ramazan Esen from Ç.U. Physics Department for XRD measurements.

REFERENCES

1. Ulusal F, Darendeli B, Erünal E, Eğitmen A, Güzel B. Supercritical carbon dioxide deposition of γ-Alumina supported Pd nanocatalysts with new precursors and using on Suzuki-Miyaura coupling reactions. The Journal of Supercritical Fluids. 2017;127:111–120.

2. Cangul B, Zhang LC, Aindow M, Erkey C. Preparation of carbon black supported Pd, Pt and Pd–Pt nanoparticles using supercritical CO2 deposition. The Journal of Supercritical Fluids. 2009; 50: 82–90.

3. Zhang Y, Erkey C. Preparation of supported metallic nanoparticles using supercritical fluids: A review. The Journal of Supercritical Fluids. 2006;38:252–267.

4. Daoush WM, Lim BK, Mo CB, Nam DH, Hong SH. Electrical and mechanical properties of carbon nanotube reinforced copper nanocomposites fabricated by electroless deposition process. Materials Science and Engineering: A. 2009;513–514:247–253.

5. Park PW, Ledford JS. The influence of surface structure on the catalytic activity of alumina supported copper oxide catalysts. Oxidation of carbon monoxide and methane. Applied Catalysis B: Environmental. 1998;15:221–231.

6. Rather S, Zacharia R, Hwang SW, Naik M, Nahm KS. Hydrogen uptake of palladium-embedded MW-CNTs produced by impregnation and condensed phase reduction method. Chemical Physics Letters. 2007;441:261–267.

7. Lam F, Hu X. A new system design for the preparation of copper/activated carbon catalyst by metal-organic chemical vapor deposition method. Chemical Engineering Science. 2003;58:687 – 695.

8. Ulusal H, Fındıkkıran G, Demirkol O, Akbaşlar D, Giray ES. Supercritical diethylether: A novel solvent for the synthesis of aryl-3,4,5,6,7,9-hexahydroxanthene-1,8-diones. The Journal of Supercritical Fluids. 2015;105:146–150.

9. Zhang Y, Erkey C. Preparation of supported metallic nanoparticles using supercritical fluids: A review. The Journal of Supercritical Fluids. 2006;38:252–267.

10. Dobrovolna Z, Kacer P, Cerveny L. Competitive hydrogenation in alkene–alkyne–

diene systems with palladium and platinum catalysts. Journal of Molecular Catalysis A: Chemical. 1998;130:279-284.

11. Ye XR, Lin Y, Whang C, Engelhard MH, Wang Y, Wai CM. Supercritical fluid synthesis and characterization of catalytic metal nanoparticles on carbon nanotubes. Journal of Materials Chemistry. 2004;14:908-913.

12. Kim J, Kelly MJ, Lamb HH, Roberts GW, Kiserow D. Characterization of palladium (Pd) on alumina catalysts prepared using liquid carbon dioxide. The Journal of Physical Chemistry C. 2008; 112: 10446–10452.

13. Erünal E, Ulusal F, Aslan MY, Güzel B, Üner D. Enhancement of hydrogen storage capacity of multi-walled carbon nanotubes with palladium doping prepared through supercritical CO2 deposition method. International Journal of Hydrogen Energy. 2018; 43: 10755-1076

14. Yildirim B, Özcan E, Deveci P. New glyoxime derivatives and their transition metal complexes. Russian Journal of Coordination Chemistry. 2007;33:417–421.

15. Teoh WH, Mammucari R, Foster NR. Solubility of organometallic complexes in supercritical carbon dioxide: A review. Journal of Organometallic Chemistry. 2013;724:102-116.

16. Aschenbrenner O, Kemper S, Dahmena N, Schaber K, Dinjus E. Solubility of β-diketonates, cyclopentadienyls, and cyclooctadiene complexes with various metals in supercritical carbon dioxide. Journal of Supercritical Fluids. 2007; 41: 179–186.

17. Guzel B, Avşar G, Çınkır H. Supercritical carbon dioxide-soluble fluorus vic-dioxime ligands and their Ni(II) complexes: synthesis, characterization and solubility properties. Synthesis and Reactivity in Inorganic, Metal-Organic, and Nano-Metal Chemistry. 2007;37:801-804.

18. Ulusal F, Güzel B. Deposition of palladium by the hydrogen assisted on SBA-15 with a new precursor using supercritical carbon dioxide. The Journal of Supercritical Fluids. 2018; 133: 233–238.

19. Cabanas A, Blackburn J, Watkins J. Deposition of Cu films from supercritical fluids using Cu(I) β-diketonate precursors. Microelectronic Engineering. 2002;64:53-61.

20. Ulusal F. Güzel B. Synthesis and Characterization of Novel Pd and Cu vic-dioxime Precursors for Their Supercritical Deposition on Multiwalled Carbon Nanotubes. Journal of the Turkish Chemical Society, Section A: Chemistry. 2018; 5(2): 635-52.